

CRYSTAL STRUCTURE AND THIRD ORDER NONLINEAR OPTICAL STUDIES ON 2-PHENYLBENZIMIDAZOLIUM- *p*-TOULENESULPHONATE

C. Sudhakar^{1,2}, M. Saravanabhavan³, M. Sekar^{2*},
B. Babu⁴, and J. Chandrasekaran⁴

A new third order nonlinear optical single crystal of 2-phenylbenzimidazolium-*p*-toulenesulphonate is grown by the solvent evaporation technique using methanol as a solvent. The single crystal X-ray diffraction analysis reveals that crystals belong to the triclinic system. A nuclear magnetic resonance and Fourier transform infrared spectroscopic study confirms the formation and vibrational analysis for the compound. UV-visible absorption studies are also carried out for the crystal. Nonlinear refractive index, absorption coefficient, and third order nonlinear optical susceptibility of the crystals are evaluated by Z-Scan studies.

DOI: 10.1134/S002247661805013X

Keywords: 2-phenylbenzimidazolium-*p*-toulenesulphonate, nonlinear refractive index, absorption coefficient, third order nonlinear optical susceptibility.

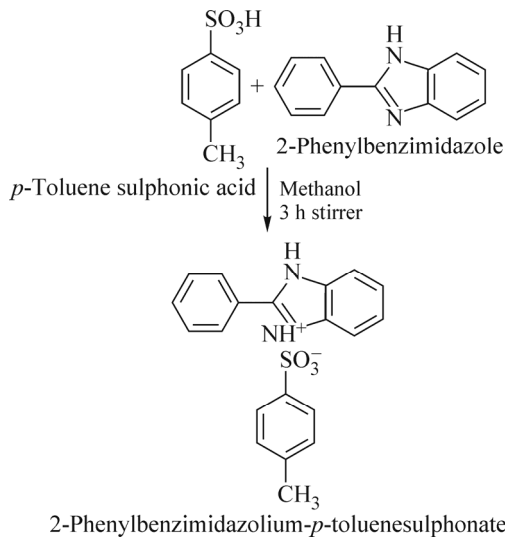
INTRODUCTION

A fascinating new field of research termed nonlinear optics was introduced to the scientific and engineering community after the invention of laser. Nonlinear optics has arisen as one of the most attractive fields of current research in view of its vital applications in optical switching, optical data storage for developing technologies in telecommunications, frequency mixing, optical parametric oscillation, optical bistability, optical logic gates, laser radiation protection, optical image processing, underwater communication, biomedical and signal processing analysis, etc. [1-5]. Organic NLO single crystals are very efficient for THz generation and high signal to noise ratio detection due to their large nonlinear optical susceptibilities and ultrafast response times [6, 7]. It has been understood that the second and third order molecular nonlinearity can be enhanced by large delocalized π -electron systems with strong donor and acceptor groups [8-10]. In the present investigation donor-acceptor based crystals of 2-phenylbenzimidazolium-*p*-toulenesulphonate (PBITS) have been grown by the slow evaporation technique and their structural, optical, and third order nonlinear optical properties were discussed in detail.

¹Research Center, Bharathiar University, Coimbatore, Tamil Nadu, India. ²Post-Graduate and Research Department of Chemistry, Sri Ramakrishna Mission Vidyalaya College of Arts and Science, Coimbatore, Tamil Nadu, India; *drmsbavan@gmail.com. ³Department of Chemistry, Dr. N.G.P. Institute of Technology, Coimbatore, Tamil Nadu, India. ⁴Post-Graduate and Research Department of Physics, Sri Ramakrishna Mission Vidyalaya College of Arts and Science, Coimbatore, Tamil Nadu, India. The text was submitted by the authors in English. *Zhurnal Strukturnoi Khimii*, Vol. 59, No. 5, pp. 1155-1162, June-July, 2018. Original article submitted July 14, 2017.

EXPERIMENTAL

Materials synthesis and growth of the PBITS single crystal. The equimolar ratio of *p*-toluenesulphonic acid in methanol and 2-phenylbenzimidazole in methanol were prepared at room temperature, mixed and stirred well for about 3 h to get a clear solution. This solution was filtered using the Whatmann 41 filter paper and kept aside unperturbed in a dust-free room for the growth of single crystals. Well defined, transparent crystals were collected at the end of the 6th day. The collected crystals were recrystallized using dry methanol to get good quality crystals. The reaction scheme and the chemical structure were illustrated.



Scheme 1. Synthesis of 2-phenylbenzimidazolium-*p*-toluenesulphonate.

Materials and instrumentation. All the chemicals were purchased from Sigma-Aldrich in the highest purity available. Solvents were purified and dried according to the standard procedure. Single crystal X-ray diffraction data of the PBITS compound were collected at room temperature on a Bruker diffractometer equipped with a fine focused sealed tube. The unit cell parameters were determined and the data on PBITS were collected using graphite-monochromated MoK_α ($\lambda = 0.71073 \text{ \AA}$) radiation by φ and ω scans. The structure of the compound was solved by the direct method using SHELXS-97, which revealed the position of all non-hydrogen atoms, and was refined by full-matrix least squares on F^2 (SHELXL-97) [11]. All non-hydrogen atoms were refined anisotropically, while the hydrogen atoms were placed in the calculated positions and refined as riding atoms. The electronic absorption spectrum was measured in methanol using a SHIMADZU 1601 UV-Vis spectrophotometer in the range 200-600 nm. In order to confirm the functional groups, the crystal was subjected to the Fourier transform infrared (FT-IR) analysis on a Perkin Elmer FT-IR 8000 spectrophotometer in the range 4000-400 cm⁻¹ using KBr pellets. To confirm the molecular structure of the compound, the ¹H and ¹³C NMR spectra were recorded employing a Bruker AV III 400 MHz spectrometer in deuterated dimethylsulfoxide as the solvent using TMS as the internal standard. The nonlinear optical measurements were carried out using a single beam Z-scan technique with a He-Ne laser operated at a repetition rate of 1 kHz and at a wavelength of 632 nm.

RESULTS AND DISCUSSION

Single crystal XRD analysis. From the X-ray diffraction studies it is known that the crystal belongs to the triclinic system with the space group *P*-1, and the lattice parameters are $a = 8.2912(5) \text{ \AA}$, $b = 9.7197(6) \text{ \AA}$, $c = 11.4293(9) \text{ \AA}$, $\alpha = 82.311(4)^\circ$, $\beta = 89.626(3)^\circ$, $\gamma = 77.915(3)^\circ$. The crystal data and details of the data collection and the structure refinement are given in Table 1. The bond lengths and bond angles of the PBITS crystal are given in Table 2 respectively. Fig. 1 shows

the ORTEP view of the molecule drawn as 50% probability thermal displacement ellipsoids with the atom numbering scheme. From the molecular structure of PBITS, we could see that there is an intermolecular hydrogen bonding between the N–H group of the 2-phenylbenzimidazolinium cation and the *P*-toluenesulfonate anion. The N atom of the 2-phenylbenzimidazole cation forms N–H...O hydrogen bonds with the O atom of the 2-phenylsulfonate anion. In the title compound the C=NH group of the 2-phenylbenzimidazole residue is engaged in the strong hydrogen bonding with the *P*-toluenesulfonate anion. The selected bond distances and angles are shown in Table 3 respectively. The molecule is stabilized by C–H...O bifurcated hydrogen bonds. All non-hydrogen atoms were refined anisotropically and the hydrogen atoms were placed in geometric positions and refined as riding atoms, except for those bound to oxygen and nitrogen atoms which were freely refined.

NMR spectral analysis. The ^1H NMR spectrum of the PBITS single crystal was recorded employing a Brucker 400 MHz spectrometer using TMS as the internal reference standard. The ^1H NMR spectrum of PBITS is depicted in Fig. 2. The singlet peak observed at δ 2.298 ppm has been assigned to three protons of the methyl group in the 2-phenylbenzoimidazolinium-*p*-toluenesulfonate. The doublet peak centered at δ 7.146 ppm ($J = 8$ Hz) is due to the C_{19} and C_{16} protons of the same kind in the aromatic ring of 2-phenylbenzoimidazolinium-*p*-toluenesulfonate. Another doublet peak centered at δ 8.226 ppm ($J = 6.8$ Hz) is due to the C_{15} and C_{20} protons of the same kind in the aromatic ring of 2-phenylbenzoimidazolinium-*p*-toluenesulfonate. The multiplet peak centered at δ 7.901–7.572 ppm is due to the C_1 , C_2 , C_3 , C_4 , C_9 , C_{10} , C_{11} , C_{12} , and C_{13} protons of the same kind of the aromatic ring of 2-phenylbenzoimidazolinium-*p*-toluenesulfonate. The NH proton appeared as singlet at δ 5.4 ppm.

The ^{13}C NMR spectrum of the PBITS single crystal was recorded employing a Brucker 400 MHz spectrometer using TMS as the internal reference. The ^{13}C NMR spectrum of PBITS is depicted in Fig. 3. The downfield carbon signal at δ

TABLE 1. Crystal Data and Structure Refinement for PBITS

Empirical formula	$\text{C}_{20} \text{H}_{18} \text{N}_2 \text{O}_3 \text{S}$
Formula weight	366.42
Temperature, K	296(2)
Wavelength, Å	0.71073
Crystal system; space group	Triclinic; $P\bar{1}$
Unit cell dimensions a , b , c , Å	8.2912(5), 9.7197(6), 11.4293(9)
α , β , γ , deg.	82.311(4), 89.626(3), 77.915(3)
Volume, Å ³	892.33(10)
Z ; calculated density, mg/cm ³	2; 1.364
Absorption coefficient, mm ⁻¹	0.204
$F(000)$	384
Crystal size, mm	0.35×0.30×0.25
θ range for data collection, deg.	1.80 to 28.36
Limiting indices h , k , l	$-11 \leq h \leq 8$, $-12 \leq k \leq 11$, $-15 \leq l \leq 15$
Reflections collected / unique	6971 / 4272 [$R(\text{int}) = 0.0167$]
Completeness to $\theta = 28.36$, %	95.9
Absorption correction	Semi-empirical from equivalents
Max. and min. transmission	0.9508 and 0.9320
Refinement method	Full-matrix least-squares on F^2
Data / restraints / parameters	4272 / 0 / 236
$Goodness-of-fit$ on F^2	1.071
Final R indices [$I > 2\sigma(I)$]	$R1 = 0.0543$, $wR2 = 0.1481$
R indices (all data)	$R1 = 0.0670$, $wR2 = 0.1642$
Largest diff. peak and hole, e/Å ³	0.643 and -0.471

TABLE 2. Bond Lengths (\AA) and Angle (deg.) for PBITS

Atoms	Bond length	Atoms	Bond Angle	Atoms	Bond Angle
S(1)–O(2)	1.4383(17)	O(2)–S(1)–O(3)	114.48(11)	C(12)–C(13)–H(13)	120.3
S(1)–O(3)	1.4562(15)	O(2)–S(1)–O(1)	114.15(12)	C(8)–C(13)–H(13)	120.3
S(1)–O(1)	1.4584(16)	O(3)–S(1)–O(1)	110.06(10)	C(11)–C(12)–C(13)	111.2(2)
S(1)–C(14)	1.772(2)	O(2)–S(1)–C(14)	106.17(11)	C(11)–C(12)–H(12)	119.4
N(1)–C(7)	1.325(3)	O(3)–S(1)–C(14)	105.48(10)	C(13)–C(12)–H(12)	119.4
N(1)–C(5)	1.397(3)	O(1)–S(1)–C(14)	105.63(9)	C(20)–C(14)–C(15)	119.2(2)
N(1)–H(1N1)	0.8600	C(7)–N(1)–C(5)	108.24(18)	C(20)–C(14)–S(1)	120.99(17)
N(2)–C(7)	1.328(3)	C(7)–N(1)–H(1N1)	125.9	C(15)–C(14)–S(1)	119.78(16)
N(2)–C(6)	1.389(3)	C(5)–N(1)–H(1N1)	125.9	C(16)–C(15)–C(14)	120.4(2)
N(2)–H(2N2)	0.8600	C(7)–N(2)–C(6)	108.24(18)	C(16)–C(15)–H(15)	119.8
C(3)–C(4)	1.383(4)	C(7)–N(2)–H(2N2)	125.9	C(14)–C(15)–H(15)	119.8
C(3)–C(2)	1.410(4)	C(6)–N(2)–H(2N2)	125.9	C(15)–C(16)–C(17)	121.0(2)
C(3)–H(3)	0.9300	C(4)–C(3)–C(2)	121.1(2)	C(15)–C(16)–H(16)	119.5
C(4)–C(5)	1.380(3)	C(4)–C(3)–H(3)	119.4	C(17)–C(16)–H(16)	119.5
C(4)–H(4)	0.9300	C(2)–C(3)–H(3)	119.4	C(16)–C(17)–C(19)	118.2(2)
C(5)–C(6)	1.378(3)	C(5)–C(4)–C(3)	115.9(2)	C(16)–C(17)–C(18)	120.5(2)
C(7)–C(8)	1.475(3)	C(5)–C(4)–H(4)	122.1	C(19)–C(17)–C(18)	121.3(2)
C(8)–C(9)	1.398(3)	C(3)–C(4)–H(4)	122.1	C(17)–C(18)–H(18A)	109.5
C(8)–C(13)	1.399(3)	C(6)–C(5)–C(4)	122.6(2)	C(17)–C(18)–H(18B)	109.5
C(9)–C(10)	1.368(4)	C(6)–C(5)–N(1)	106.4(2)	H(18A)–C(18)–H(18B)	109.5
C(9)–H(6)	0.9300	C(4)–C(5)–N(1)	131.0(2)	C(17)–C(18)–H(18C)	109.5
C(10)–C(11)	1.364(4)	N(1)–C(7)–N(2)	110.2(2)	H(18A)–C(18)–H(18C)	109.5
C(10)–H(10)	0.9300	N(1)–C(7)–C(8)	124.95(19)	H(18B)–C(18)–H(18C)	109.5
C(11)–C(12)	1.363(4)	N(2)–C(7)–C(8)	124.81(19)	C(14)–C(20)–C(19)	119.9(2)
C(11)–H(11)	0.9300	C(9)–C(8)–C(13)	118.8(2)	C(14)–C(20)–H(20)	120.1
C(2)–C(1)	1.364(4)	C(9)–C(8)–C(7)	120.9(2)	C(19)–C(20)–H(20)	120.1
C(2)–H(2)	0.9300	C(13)–C(8)–C(7)	120.3(2)	C(17)–C(19)–C(20)	121.3(2)
C(1)–C(6)	1.379(3)	C(10)–C(9)–C(8)	119.9(2)	C(17)–C(19)–H(19)	119.3
C(1)–H(1)	0.9300	C(10)–C(9)–H(6)	120.0	C(20)–C(19)–H(19)	119.3
C(13)–C(12)	1.369(4)	C(8)–C(9)–H(6)	120.0		
C(13)–H(13)	0.9300	C(11)–C(10)–C(9)	120.7(2)		
C(12)–H(12)	0.9300	C(11)–C(10)–H(10)	119.6		
C(14)–C(20)	1.381(3)	C(9)–C(10)–H(10)	119.6		
C(14)–C(15)	1.384(3)	C(12)–C(11)–C(10)	120.0(2)		
C(15)–C(16)	1.379(3)	C(12)–C(11)–H(11)	120.0		
C(15)–H(15)	0.9300	C(10)–C(11)–H(11)	120.0		
C(16)–C(17)	1.383(3)	C(1)–C(2)–C(3)	122.1(3)		
C(16)–H(16)	0.9300	C(1)–C(2)–H(2)	119.0		
C(17)–C(19)	1.384(4)	C(3)–C(2)–H(2)	119.0		
C(17)–C(18)	1.510(4)	C(2)–C(1)–C(6)	116.4(2)		
C(18)–H(18A)	0.9600	C(2)–C(1)–H(1)	121.8		
C(18)–H(18B)	0.9600	C(6)–C(1)–H(1)	121.8		
C(18)–H(18C)	0.9600	C(5)–C(6)–C(1)	121.9(2)		
C(20)–C(19)	1.385(4)	C(5)–C(6)–N(2)	106.9(2)		
C(20)–H(20)	0.9300	C(1)–C(6)–N(2)	131.2(2)		
C(19)–H(19)	0.9300	C(12)–C(13)–C(8)	119.5(2)		

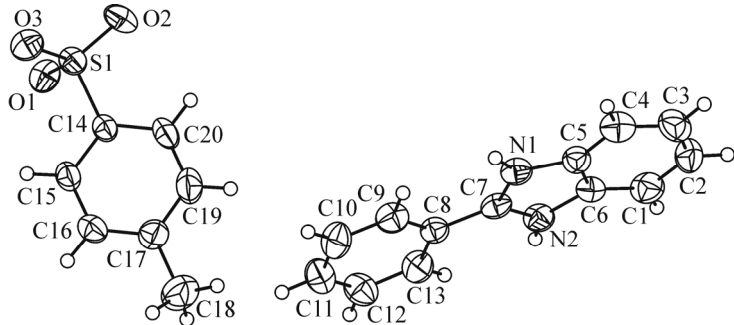


Fig. 1. ORTEP diagram of PBITS.

TABLE 3. Hydrogen Bond for PBITS

D–H...A	<i>d</i> (D–H)	<i>d</i> (H...A)	\angle DHA	<i>d</i> (D...A)	Symmetry
N1–H1N1...O1	0.860	1.82	170	2.674	$x, y, z+1$
N2–H2N2...O3	0.860	1.87	160	2.691	$x, -1+y, 1+z$
C9–H6...O1	0.930	2.56	160	3.450	$x, y, 1+z$
C16–H16...O2	0.930	2.54	156	3.410	$-1+x, y, z$
C20–H20...O2	0.930	2.51	105	2.892	

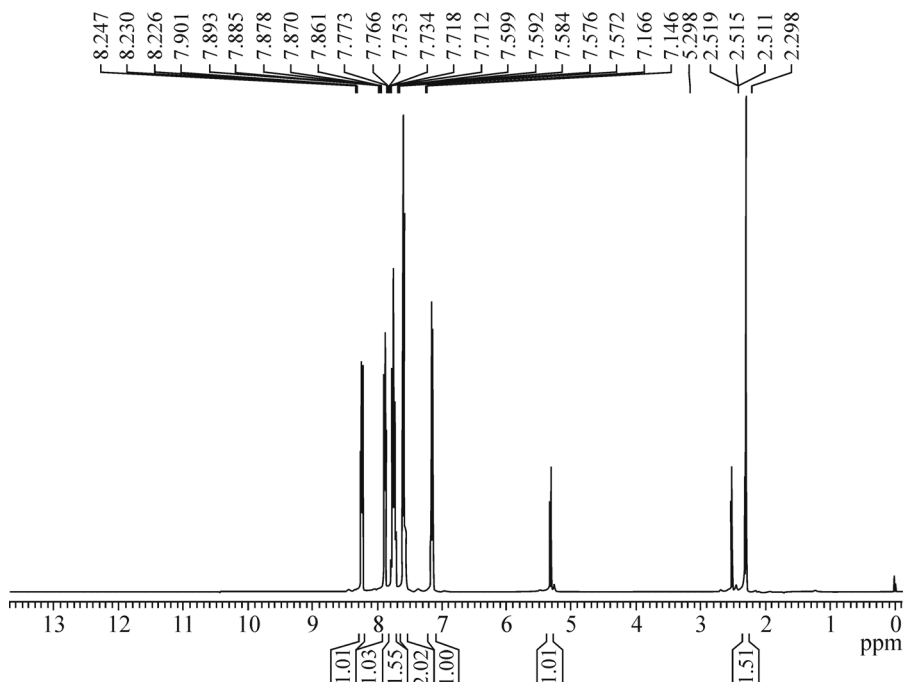


Fig. 2. ^1H NMR spectrum of PBITS.

154.25 ppm corresponds to the C_7 carbon atom of the 2-phenylbenzimidazole moiety. The carbon signal at δ 150.22 ppm belongs to the C_{14} carbon atom of the *p*-toluenesulfonic acid moiety. The carbon signal at δ 143.41 ppm corresponds to the C_5 carbon atom of the *p*-toluenesulfonic acid moiety. The carbon signal at δ 138.63 ppm belongs to the C_4 carbon atom of the 2-phenylbenzimidazole moiety. The sharp and intense signal at δ 137.06 ppm is due to the C_{15} and C_{20} carbon atoms of the same kind in the *p*-toluenesulfonic acid moiety. The carbon signal at δ 134.94 ppm corresponds to the C_8 and C_{11} carbon atoms of the 2-phenylbenzimidazole moiety. The sharp and intense signal at δ 133.20 ppm is due to the C_9 and C_{13} carbon atoms of the same kind in the 2-phenylbenzimidazole moiety. The carbon signal at δ 131.28 ppm belongs to the C_{10} and C_{12}

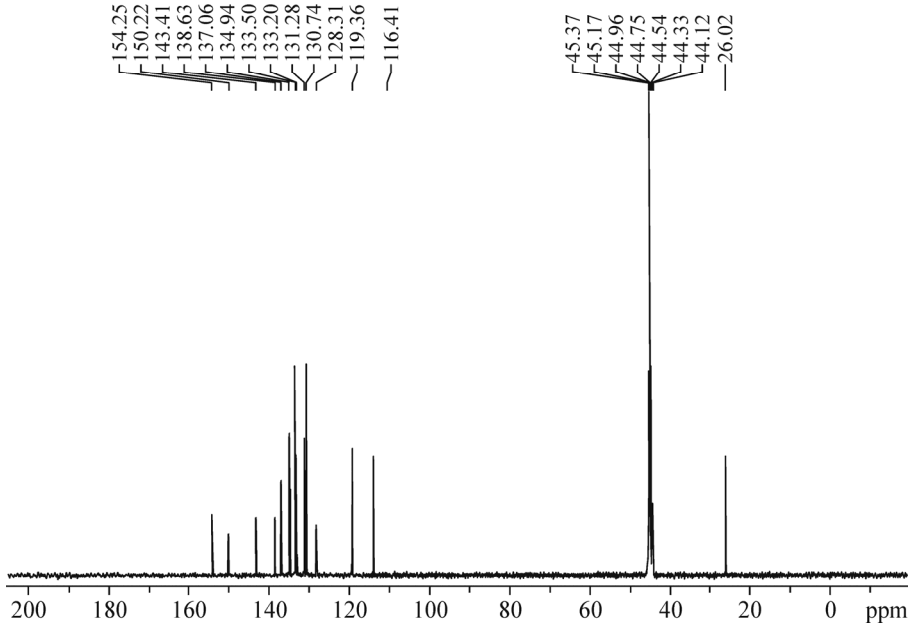


Fig. 3. ^{13}C NMR spectrum of PBITS.

carbon atoms of the 2-phenylbenzimidazole moiety. The carbon signal at δ 130.74 ppm corresponds to the C₁₆ and C₁₉ carbon atoms of the 2-phenylbenzimidazole moiety. The sharp and intense signal at δ 128.31 ppm is due to the C₂ and C₃ carbon atoms of the same kind in the *p*-toluenesulfonic acid moiety. The sharp and intense signal at δ 119.36 ppm is due to the C₁₇ carbon atom of the same kind in the 2-phenylbenzimidazole moiety. The carbon signal at δ 26.02 ppm corresponds to the methyl carbon atom of the 2-phenylbenzimidazole moiety.

FT-IR spectral studies. The FT-IR spectrum of the PBITS crystal was recorded employing a Perkin ElmerFT-IR spectrometer using the KBr pellet technique in the range 4000–400 cm^{-1} and the FT-IR spectrum of the PBITS crystal is depicted in Fig. 4. The recorded FT-IR spectrum was analyzed to ascertain the functional groups present in the compound. The formation of PBITS during the reaction between *p*-toluenesulfonic acid and 2-phenylbenzimidazole is strongly evidenced by the presence of the main characteristic IR band in the crystal. The formation of PBITS is evidenced by the presence of the most prominent group in the PBITS crystal, such as N–H, C–H, C=N, C–N, and SO₂ groups. The band observed at 3336 cm^{-1} is due to the N–H symmetric stretching vibration. The aromatic C–H stretching vibration is observed at 3062 cm^{-1} , 2930 cm^{-1} , and 2853 cm^{-1} . The band observed at 1634 cm^{-1} indicates the presence of the C=N group in the PBITS molecule. The aromatic C–H bending vibration is observed at 1457 cm^{-1} . The 1396 cm^{-1} band indicates the presence of the C–N stretching vibration in the molecule. The sharp band observed at 1166 cm^{-1} indicates the presence of the aromatic SO₂ symmetric stretching vibration.

Electronic absorption spectroscopic studies. The UV-visible absorption spectrum of the PBITS crystal was recorded employing a SYSTRONICS double beam spectrophotometer 2202 in a range from 200 nm to 600 nm using DMSO as a solvent, and the spectrum is shown in Fig. 5. From the spectrum, it is observed that the compound exhibits two characteristic absorption bands. The bands at about 296.0 nm and 329.6 nm are assigned to the $\pi \rightarrow \pi^*$ transition of the title compound. Also the absence of absorption in the region between 330 nm and 600 nm makes the crystal suitable for optical applications [7, 12].

Z-scan studies. The Z-scan is a well-known experimental technique to measure the intensity dependent third order nonlinear susceptibility of the materials [13, 14]. The open and closed aperture Z-scan configurations are used to investigate the nonlinear absorption coefficient β and the nonlinear refractive index n_2 . Fig. 6a shows the normalized transmittance T with a closed aperture as a function of the distance z along the lens axis in the far field. Fig. 6b shows the normalized

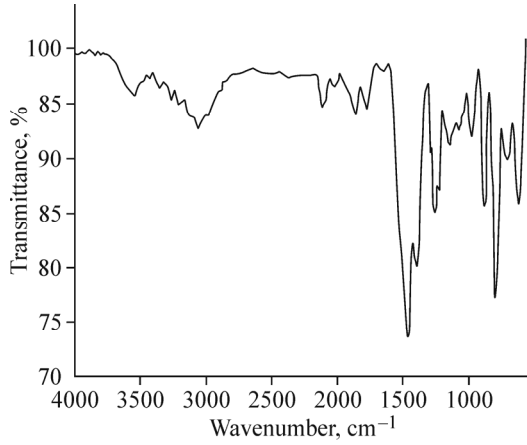


Fig. 4. FT-IR spectrum of PBITS.

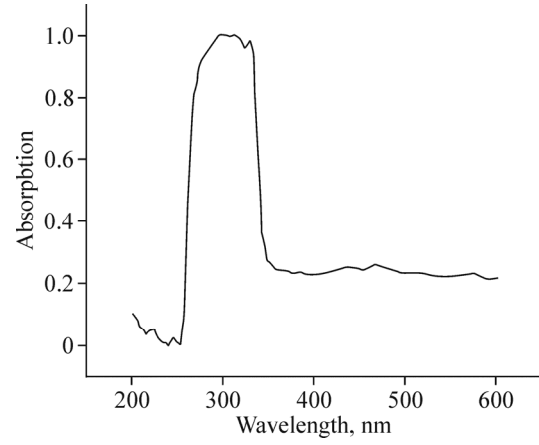


Fig. 5. Electronic absorption spectrum of PBITS.

transmittance with an open aperture as a function of the distance z along the lens axis in the far field. The nonlinear refractive index n_2 of the crystal was calculated using the standard relation given below

$$\Delta\phi_0 = \frac{\Delta T_{p-v}}{0.406(1-s)^{0.25}}, \quad (1)$$

where ΔT_{p-v} is the difference between the normalized peak and valley transmittance and s is the linear transmittance of the aperture. The nonlinear refractive index n_2 and the nonlinear absorption coefficient β are given by

$$n_2 = \frac{\Delta\phi}{kI_0L_{\text{eff}}}, \quad (2)$$

$$\beta = \frac{2\sqrt{2}\Delta T}{I_0L_{\text{eff}}}, \quad (3)$$

where k is the wavenumber; $k = 2\pi/\lambda$ and

$$L_{\text{eff}} = \frac{1 - e^{(-\alpha L)}}{\alpha}, \quad (4)$$

with $I_0 = \frac{P}{\pi\omega_0^2}$ defined as the peak intensity within the sample, where L_{eff} is the sample thickness and α is the linear absorption coefficient. The real and imaginary parts of the third order nonlinear susceptibility $\chi(3)$ are defined as

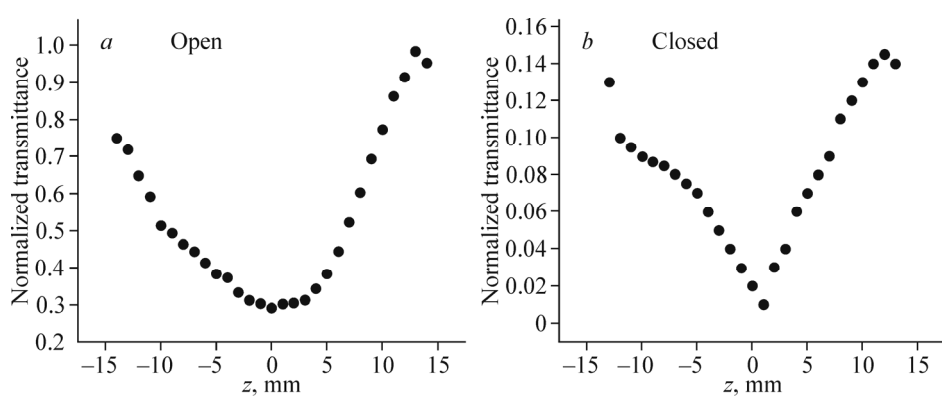


Fig. 6. Normalized transmittance with open (a) and closed (b) aperture.

$$\text{Re}\chi^{(3)} = 10^{-4} \frac{(\epsilon_0 C^2 n_0^2 n^2)}{\pi(\text{esu})}, \quad (5)$$

$$\text{Im}\chi^{(3)} = 10^{-2} \frac{(\epsilon_0 C^2 n_0^2 \lambda \beta)}{4\pi^2(\text{esu})}, \quad (6)$$

where ϵ_0 is the vacuum permittivity; n_0 is the linear refractive index of the sample, and c is the velocity of light in vacuum. Thus, we can easily obtain the absolute value of $\chi(3)$ using the following formula:

$$|\chi^{(3)}| = [(\text{Re}\chi^{(3)})^2 + (\text{Im}\chi^{(3)})^2]^{1/2}. \quad (7)$$

As seen from the closed aperture Z scan curve, the prefocal transmittance valley is followed by the post focal peak, which is the positive nonlinearity [15]. The calculated value of the nonlinear refractive index n_2 is $6.40149 \cdot 10^{-8} \text{ cm}^2/\text{W}$. The value of the nonlinear absorption coefficient β estimated from the open aperture Z-scan curve is $2.4603 \cdot 10^{-4} \text{ cm/W}$. The third order susceptibility of PBITS is $1.3061 \cdot 10^{-7} \text{ esu}$. Since the material has a positive refractive index, it results in the self-focusing nature of the material, which is an essential property for all optical switching devices [16].

CONCLUSIONS

A new bright, transparent organic compound PBITS was synthesized and the crystal was grown by the slow evaporation solution growth method at room temperature. The material synthesized was characterized by various analytical, spectroscopic, and single crystal XRD studies. From the X-ray diffraction studies of the PBITS single crystal it is observed that the crystal belongs to the triclinic system with the space group $P-1$. The UV-visible absorption spectrum confirms the suitability of the title crystal for various optical applications. The molecular structure of the compound was confirmed by the FT-IR, ^1H and ^{13}C NMR spectral studies. Z-scan studies reveal the self-focusing nature of the material, which is a vital property for all optical switching and optical limiting applications.

REFERENCES

1. B. Babu, J. Chandrasekaran, R. Thirumurugan, V. Jayaramakrishnan, and K. Anitha. *J. Mater. Sci: Mater. Electron.*, **2016**, 1.
2. A. Majchrowski, I. V. Kityk, T. Łukasiewicz, A. Mefleh, and S. Benet. *Opt. Mater.*, **2000**, 15, 51.
3. V. Subhashini, S. Ponnusamy, and C. Muthamizhchelvan. *Spectrochim. Acta, Part A*, **2012**, 87, 265.
4. G. Saravana Kumar and P. Murugakoothan. *Optik*, **2015**, 126, 68.
5. S. A. Martin Britto Dhas and S. Natarajan. *Opt. Commun.*, **2008**, 281, 457.
6. G. Peramaiyan, P. Pandi, B. M. Sornamurthy, G. Bhagavannarayana, and R. Mohan Kumar. *Spectrochim. Acta, Part A*, **2012**, 95, 310.
7. K. Thirupugalmani, S. Karthick, G. Shanmugam, V. Kannan, B. Sridhar, K. Nehru, and S. Brahadeeswaran. *Opt. Mater.*, **2015**, 49, 158.
8. D. S. Chemla and J. Zyss. Nonlinear Optical Properties of Organic molecules and crystals, 1-2. Orlando, New York: Academic Press, **1987**.
9. M. Suresh, S. Asath Bahadur, and S. Athimoolam. *J. Mol. Struct.*, **2016**, 1112, 63.
10. J. Mohana, G. Ahila, M. Divya Bharathi, and G. Anbalagan. *J. Cryst. Growth*, **2016**, 450, 181.
11. G. M. Sheldrick. SHELXL97 and SHELXS97. University of Gottingen, Germany, **1997**.
12. B. Babu, J. Chandrasekaran, and S. Balaprabhakaran. *Optik*, **2014**, 125, 3005.
13. M. Sheik-Bahae, A. A. Said, and E. W. Van Stryland. *Opt. Lett.*, **1989**, 17, 955.
14. M. Sheik-Bahae, A. A. Said, T. H. Wei, D. J. Hagan, and E. W. Van Stryland. *IEEE J. Quant. Elect.*, **1990**, 26, 760.
15. S. L. Gomez, F. L. S. Cuppo, and A. M. Figueiredo Neto. *Braz. J. Phys.*, **2003**, 33, 813.
16. M. Sheik, C. H. David, D. J. Hagan, and E. W. Van Stryland. *IEEE J. Quantum Electron.*, **1991**, 27, 1296.